Current Biology 22, 437–444, March 6, 2012 ©2012 Elsevier Ltd All rights reserved DOI 10.1016/j.cub.2012.01.041

Report

Anaphase B Precedes Anaphase A in the Mouse Egg

Greg FitzHarris[1,*]
[1]University College London Institute for Women's Health, 86–96 Chenies Mews, London WC1E 6HX, UK

Summary

Segregation of chromosomes at the time of cell division is achieved by the microtubules and associated molecules of the spindle. Chromosomes attach to kinetochore microtubules (kMTs), which extend from the spindle pole region to kinetochores assembled upon centromeric DNA. In most animal cells studied, chromosome segregation occurs as a result of kMT shortening, which causes chromosomes to move toward the spindle poles (anaphase A). Anaphase A is typically followed by a spindle elongation that further separates the chromosomes (anaphase B) [1–5]. The experiments presented here provide the first detailed analysis of anaphase in a live vertebrate oocyte and show that chromosome segregation is initially driven by a significant spindle elongation (anaphase B), which is followed by a shortening of kMTs to fully segregate the chromosomes (anaphase A). Loss of tension across kMTs at anaphase onset produces a force imbalance, allowing the bipolar motor kinesin-5 to drive early anaphase B spindle elongation and chromosome segregation. Early anaphase B spindle elongation determines the extent of chromosome segregation and the size of the resulting cells. The vertebrate egg therefore employs a novel mode of anaphase wherein spindle elongation caused by loss of k-fiber tension is harnessed to kick-start chromosome segregation prior to anaphase A.

Results and Discussion

Anaphase B Occurs Prior to Anaphase A in Mouse Eggs and Determines Cell Size

To begin to understand the mechanism of anaphase in oocytes, real-time examination of microtubules and chromosomes was performed in mouse meiosis II eggs. Prior to chromosome segregation, the metaphase spindle was 27 ± 0.7 μm in length. Chromosome separation began 10–20 min after parthenogenetic egg activation (Figure 1). Strikingly, a marked elongation of the spindle occurred concomitantly with the initiation of anaphase onset in all eggs examined, during which the spindle reached 35.2 ± 0.8 μm (30% ± 2% length increase). During this initial period, poleward movement of the chromosomes was relatively minor, and comparison of overall chromatid separation and the chromosome-pole distance revealed that spindle elongation accounted for the majority of chromosome movement (~75% contribution). Following the spindle elongation, chromosome segregation was completed by poleward chromosome movement (anaphase A). There was no further change in spindle length once the chromosomes arrived at spindle poles, and spindle length and chromosome separation distance remained constant throughout cytokinesis and polar body formation (see Figure S1 available online). Thus, anaphase in eggs is first driven by a marked spindle elongation (anaphase B), which is followed by anaphase A poleward chromosome motion that completes chromosome segregation.

Next, experiments were designed to dissect the mechanism of early-anaphase spindle elongation. Given the recent descriptions of interactions between actin microfilaments and spindle microtubules in mouse oocytes [6–8] and of the ability of microfilaments to influence spindle morphology [9], the involvement of microfilaments was tested. As expected, the actin-depolymerizing agent cytochalasin B removed the cortical actin cap characteristic of eggs and prevented polar body formation, demonstrating effective microfilament disruption (data not shown). However, cytochalasin B did not prevent early-anaphase spindle elongation (33% ± 3% elongation) or have any effect upon chromosome separation velocity (Figure 2A).

In addition to kinetochore microtubules (kMTs) that attach chromosomes, spindles possess interpolar microtubules (ipMTs) that extend beyond the chromosomes, causing antiparallel microtubules to overlap. In vertebrate eggs, the bipolar plus-end-directed motor kinesin-5 contributes to steady-state spindle length by sliding overlapping antiparallel MTs poleward, thereby generating an "outward" force that maintains the pole-pole distance in metaphase [10–12]. This contrasts with mammalian somatic cells, where kinesin-5 is largely dispensable for spindle length in metaphase [10, 13–15]. To determine whether kinesin-5 contributes to early anaphase spindle elongation, eggs were treated with monastrol, which has been validated as a reliable kinesin-5 inhibitor in a variety of systems, including mouse oocytes [12, 16, 17]. In contrast to metaphase, monastrol did not cause spindle collapse in anaphase. However, monastrol significantly suppressed early-anaphase spindle elongation: monastrol-treated spindles elongated by only 14% ± 2% of their original length ($p < 0.001$). Chromosomes nonetheless moved to spindle poles, suggesting that anaphase A was unaffected (Figure 2A). Thus, although other mechanisms may also participate, kinesin-5 makes a major contribution to early-anaphase spindle elongation. Consistent with a failure of spindle elongation, polar bodies formed by monastrol-treated oocytes were significantly smaller than controls ($p < 0.001$; Figure 2B). Therefore, the early anaphase B determines the final extent of chromosome segregation and thereby dictates the size of the resulting cell (the polar body).

Chromosome Disjunction Triggers Early Anaphase B

In some systems, interventions that interfere with chromosome cohesion or with MT-kinetochore interactions cause metaphase spindle lengthening, suggesting that "outward" spindle forces place kMTs under tension in metaphase and k-fiber tension exerts an "inward" force restricting metaphase spindle length [18–23]. Given that early-anaphase spindle elongation occurs at the onset of anaphase, when sister chromatid cohesion is lost, and given that kinesin-5 is necessary both for spindle length maintenance in metaphase and for elongation in anaphase, it was reasoned that early-anaphase

*Correspondence: g.fitzharris@ucl.ac.uk

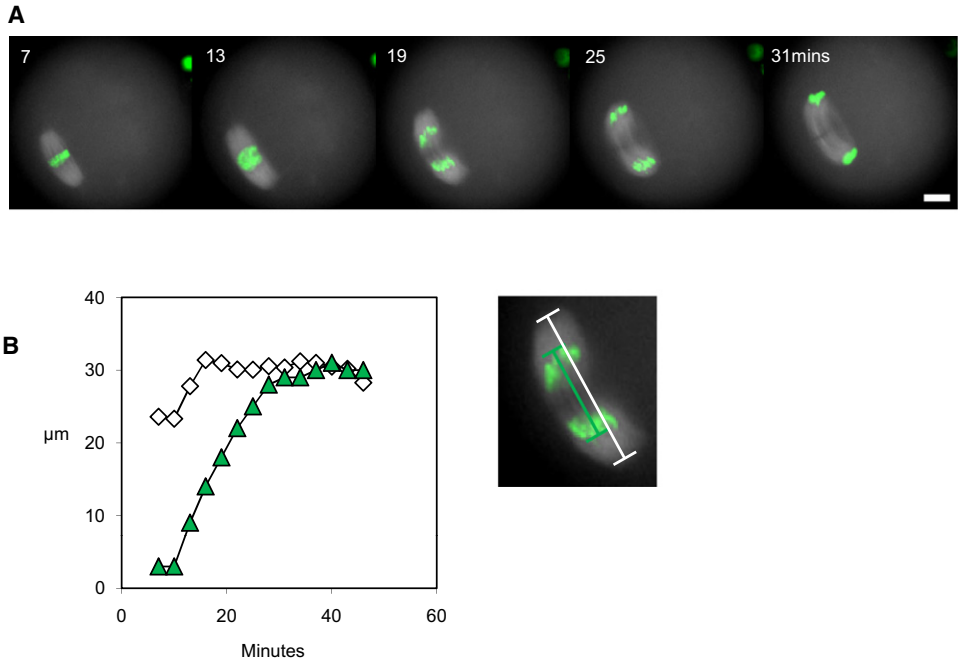

Figure 1. Anaphase in the Mouse Egg

(A) Time-lapse imaging of microtubules (MAP7-GFP, gray) and chromosomes (green) at times indicated following parthenogenesis. Scale bar represents 10 μm.

(B) Analysis of spindle length and chromosome separation distance during anaphase in the example shown in (A). Zoomed image illustrates measurements made. n = 19 oocytes from six experiments.

spindle elongation may reflect a loss of force-balance equilibrium after sister cohesion and k-fiber tension are lost. This hypothesis makes three testable predictions. First, kinesin-5 should participate in placing chromosomes under tension in metaphase. Second, failure of chromosome disjunction should prevent anaphase spindle elongation. Third, loss of chromosome cohesion should cause metaphase spindle lengthening.

To investigate whether chromosomes are under tension in metaphase, the effect of the MT-destabilizing agent nocodazole was examined. Nocodazole causes rapid loss of ipMTs and decreases overall spindle MT density [24] (Figures 3A and S2). Five minutes after nocodazole addition, sister kinetochores were substantially closer together than in controls, revealing that, as in other systems [25, 26], chromosomes are under tension in metaphase eggs. To directly assess the role of kinesin-5, a similar experiment was performed using monastrol. As previously, monastrol caused spindle shortening without loss of spindle MT density [12]. Ten minutes of monastrol treatment substantially shortened interkinetochore distance ($p < 0.01$; Figure 3A). Thus, kinesin-5 contributes to placing chromosomes under tension and maintaining interkinetochore spacing in metaphase eggs.

Next, an experiment was performed to determine whether preventing chromosome disjunction would inhibit early-anaphase spindle elongation. Sister chromatid cohesion in metaphase is maintained by cohesins. Anaphase chromatid disjunction is permitted by destruction of the separase inhibitor securin, which frees separase to cleave cohesin subunits (reviewed in [27]). Therefore, to prevent loss of chromosome cohesion at anaphase, a YFP-tagged securin containing D box and KEN box mutations that render it indestructible by the anaphase-promoting complex pathway ($^{\Delta D\text{-box/KEN-box}}$securin-YFP) [28] was employed. Parthenogenetically activated $^{\Delta D\text{-box/KEN-box}}$securin-YFP eggs failed to extrude a polar body in most cases but formed pronuclei with approximately normal timing, confirming M phase exit. Spindle microtubules underwent morphological changes characteristic of anaphase, including formation of a dense and constricted spindle midzone prior to chromosome decondensation and pronucleus formation (Figure 3B). Consistent with a failure to cleave cohesins, chromosomes failed to segregate to spindle poles normally. However, the characteristic spindle elongation that normally follows egg activation was never observed (Figure 3B). Thus, the ability to segregate sisters is necessary to achieve anaphase spindle elongation.

Finally, to test the prediction that artificially triggering chromatid disjunction might cause spindle elongation, eggs were microinjected with morpholino antisense oligonucleotides that cause specific and efficient depletion of securin in mouse eggs (securin-MO) [29, 30]. Colabeling kinetochores and DNA confirmed that securin-MO caused sister chromatid disjunction (Figure 3C), as previously [29]. Notably, spindles in securin-MO-injected oocytes were substantially elongated compared to controls ($p < 0.01$), with poles contacting the plasmalemma in all cases, and chromatids at apparently random positions along the spindle (Figure 3C). Contemporaneous controls injected with a nonspecific MO sequence (control-MO) were of normal length and appearance. Monastrol caused spindle collapse in securin-MO eggs, suggesting that kinesin-5 continues to exert an outward force after chromatid disjunction and that further spindle elongation is limited by the plasmalemma (Figure S2B). Cold-shock treatment (see Experimental Procedures), which allows preferential

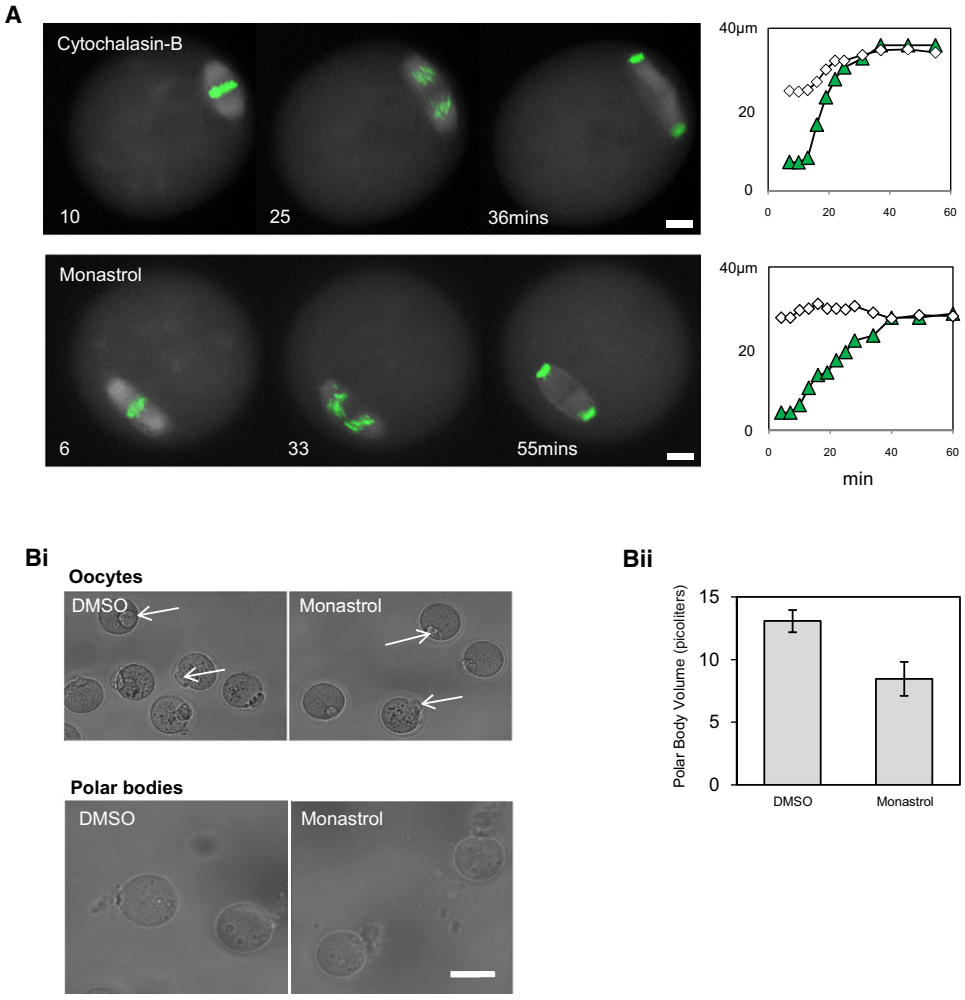

Figure 2. Anaphase B Spindle Elongation Is Kinesin-5 Dependent

(A) Anaphase in the presence of cytochalasin B or monastrol. Colors are as in Figure 1. Reagents were added immediately after parthenogenesis. Note that whereas cytochalasin B-treated eggs (5 μg/ml; n = 11) undergo early-anaphase spindle elongation and segregate chromosomes similar to untreated oocytes, monastrol (200 μM) significantly suppresses spindle elongation (n = 15; see text).

(Bi) Bright-field images of oocytes activated in the presence or absence of monastrol. Arrows indicate polar bodies. Bottom panels show second polar bodies isolated from oocytes in the same experiment to calculate volume (see Experimental Procedures).

(Bii) Polar bodies were significantly smaller following monastrol treatment ($p < 0.001$, Student's t test).

Scale bars represent 10 μm. Error bars indicate SEM.

visualization of stable MTs, revealed that whereas control-MO spindles possessed kMT bundles stretching from poles to the kinetochores, as expected, securin-MO spindles possessed faint arrays of MTs with laterally associated chromosomes (Figure 3C). Therefore, experimentally inducing sister chromatid disjunction produces spindles without kMTs that undergo an elongation, consistent with a role for kMTs in restraining spindle length. The extent of spindle elongation in these experiments (~60% elongation) was greater than the ~30% elongation at anaphase. This likely reflects the lack of a cyclin B/cdk1 activity decrease, which limits spindle elongation in anaphase in mitosis [31]. In summary, these experiments are all consistent with a model in which kinesin-5 and interpolar MT-dependent forces place kMTs under tension in metaphase. The imbalance of forces that is created by the loss of kMT tension triggers the early-anaphase B spindle elongation, which in turn powers the initial phase of chromosome separation.

kMTs Disassemble at Both Ends during Anaphase A

Experiments were next designed to determine the mechanism of poleward chromosome motion (anaphase A). Anaphase A kMT shortening can occur by MT disassembly at spindle poles, and also at kinetochores (termed "pacman"). In somatic cells, the relative contribution of MT disassembly at the pole is typically ~1/3, and pacman is ~2/3 [32–35]. However, in meiosis II *Xenopus* oocyte homogenates and in insect spermatocytes, anaphase A is primarily accounted for by MT disassembly at the pole [26, 36–38], suggesting that pacman may be of relatively minor importance in meiosis. In anaphase mouse eggs, following cold-shock treatment, microtubule bundles were evident linking the spindle pole to the kinetochore, with the kinetochore found at the leading edge of the chromosome (Figure 4A), consistent with kMT shortening being the means of anaphase A chromosome motion. To determine the site of kMT shortening in anaphase, photoactivatable GFP::tubulin (PAGFP::tubulin) was expressed in

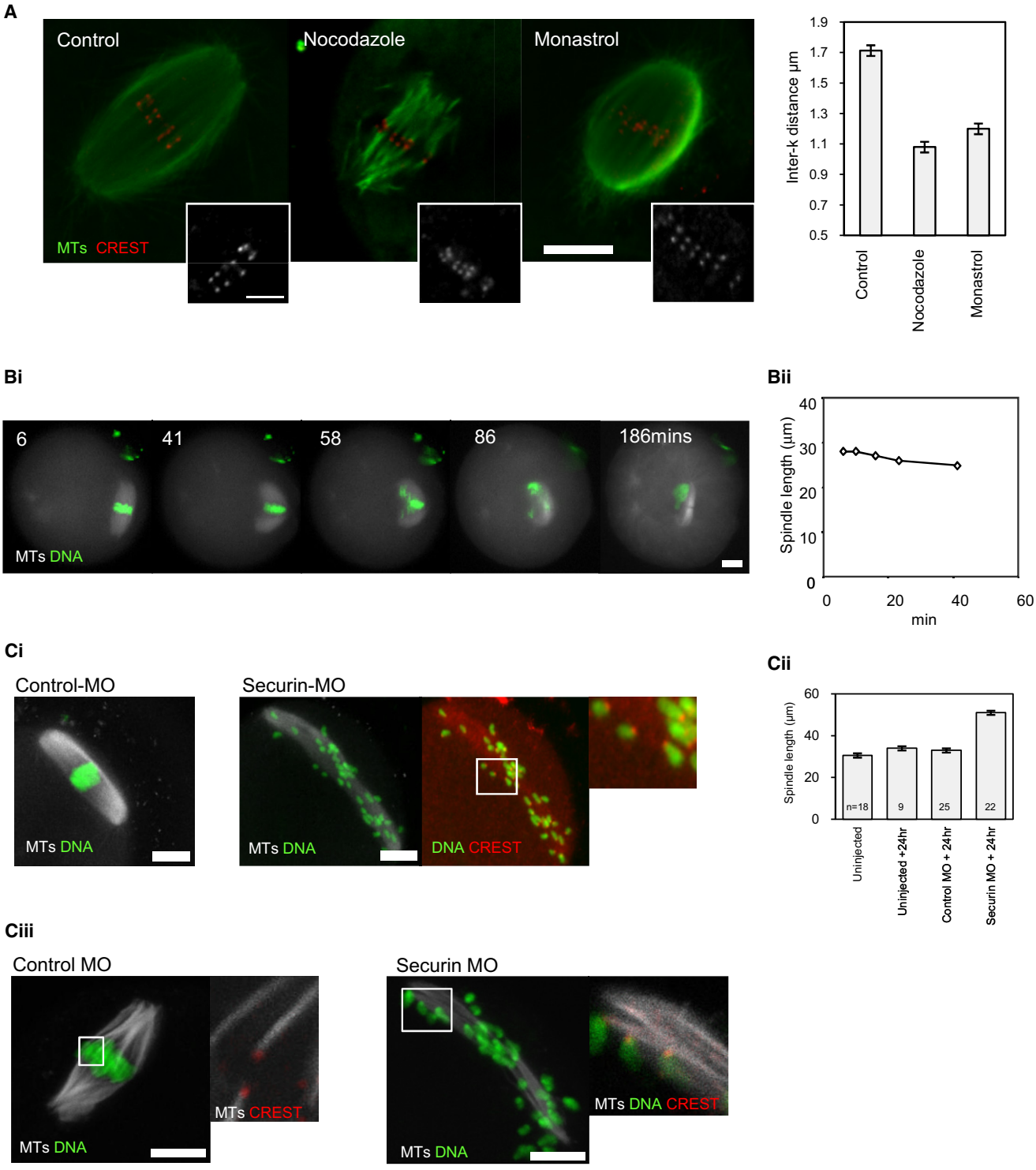

Figure 3. Evidence that Chromosome Disjunction Triggers Anaphase Spindle Elongation

(A) Kinesin-5 contributes to placing chromosomes under tension in metaphase. Eggs were treated with nocodazole (10 µM, 5 min) or monastrol (200 µM, 10 min) prior to fixation. Interkinetochore distance was measured for seven or more kinetochore pairs per oocyte in a minimum of ten oocytes per treatment group. Insets show typical single confocal slices of CREST-labeled kinetochores used for interkinetochore distance measurements. MT brightness has been increased in the nocodazole-treated example to allow visualization of the remaining microtubules. Either treatment significantly decreased interkinetochore spacing compared to untreated controls (analysis of variance, Tukey, $p < 0.01$).

(Bi and Bii) Nondegradable securin prevents early-anaphase spindle elongation.

(Bi) Time-lapse microscopy of microtubules (MAP7-RFP, gray) and chromosomes (green) in $^{\Delta D\text{-box/KEN-box}}$securin-YFP-expressing eggs following parthenogenetic activation.

(Bii) Analysis of spindle length following egg activation. Note that the spindle lengthening normally associated with anaphase does not occur in $^{\Delta D\text{-box/KEN-box}}$ securin-YFP-expressing eggs.

eggs. PAGFP::tubulin allows a subgroup of spindle microtubules to be selectively labeled and their location subsequently monitored using GFP fluorescence [39]. A line of photoactivated PAGFP::tubulin was created between the chromatin and spindle poles in anaphase A by brief targeted exposure to 405 nm light. The overall velocity of chromosome movement in these experiments was similar to the epifluorescence imaging experiments, confirming that photoactivation and confocal imaging did not impair anaphase. The PAGFP bar moved poleward during anaphase at 0.25 ± 0.03 μm/min, revealing continued disassembly at spindle poles in anaphase, albeit at a slower rate than in metaphase (~0.5–0.6 μm/min [12]). The distance between the chromosomes and the PAGFP bar progressively shortened at a rate of 0.35 ± 0.03 μm/min during anaphase A, indicating that kMT depolymerization at the kinetochore plays a major role in anaphase movement (Figure 4B). Thus, unlike in other meiotic systems studied to date, disassembly of MTs at the kinetochore makes a major contribution to anaphase A.

Understanding the mechanisms of chromosome segregation in oocytes is clinically important because segregation errors are relatively common in mammalian oocytes, both in meiosis I and in meiosis II, and lead to embryonic aneuploidy and pregnancy loss [40, 41]. Recent elegant experiments in *C. elegans* oocytes revealed that anaphase proceeds by a kMT-independent mechanism, leading to the proposal that anaphase may be highly specialized in oocytes across species [42]. In contrast, the present study suggests that anaphase in mammalian oocyte meiosis II employs a kMT-led mechanism. This has important ramifications for our understanding of the etiology of segregation errors because mechanisms of error correction in somatic cells may also be relevant in the mammalian oocyte. Whether the same mechanisms underpin anaphase in meiosis I is yet to be determined.

The experiments presented here provide a demonstration of the postulated role of tension across kMT fibers as a determinant of spindle length [22, 23]. This is supported here by three complementary observations: (1) anaphase spindle elongation occurs concomitant with loss of sister cohesion, (2) persistent cohesion prevents elongation, and (3) experimentally induced loss of cohesion causes spindle elongation. The loss of tension at anaphase onset thus causes a sudden increase in spindle length, causing anaphase B to precede anaphase A (see Figure 4C). That the loss of k-fiber tension is converted into an early anaphase B in eggs may be a reflection of cell size; the proximity of spindle poles to the plasmalemma and interactions of astral MTs with the cortex may limit early-anaphase spindle elongation in mitosis, whereas the size of the egg permits early-anaphase elongation. Alternatively, the elongation may reflect the importance of kinesin-5 in oocyte spindles. The reliance of metaphase length maintenance upon kinesin-5 in oocytes, in contrast to mitosis where kinesin-5 is largely dispensable for metaphase spindle length maintenance [10, 13–15], may prime the spindle for the unusual elongation that drives the first steps of chromosome segregation. Alternatively, more detailed analyses of spindle length in anaphase may unearth a similar mechanism in other cell types. It is concluded that the spindle of the oocyte in mammals, unlike in lower species [42], has employed much of the same machinery and principles as the somatic cell but has used them atypically, resulting in an unexpected back-to-front anaphase.

Experimental Procedures

Materials and Oocyte Handling

MF1 mice were superovulated by sequential intraperitoneal injections of pregnant mare's serum gonadotropin (PMSG) and human chorionic gonadotropin (hCG) at a 48 hr interval, and eggs were collected from the oviducts. Experiments were carried out under a project license issued by the UK Home Office. All egg handling and live imaging was carried out in M2 medium at 37°C and overnight culture in M16 medium. To initiate anaphase, parthenogenesis was performed using 7% ethanol for 7 min at 25°C at 18–20 hr post hCG. To calculate polar body volume, the zona pellucida was removed using warmed acidified Tyrode's solution (Sigma). Zona-free oocytes were then pipetted using a narrow pipette, which lysed the oocyte, leaving the polar body intact. Repeated pipetting allowed the vast majority of the ooplasm to be removed. Bright-field images were then taken of the rounded polar bodies, and volume was calculated from the measured diameter.

Manufacture and Microinjection of mRNA

Photoactivatable GFP::tubulin [39] was purchased in the pIREShyg vector from Addgene. MAP7-GFP and MAP7-RFP were used previously [12] and were a kind gift from Alex McDougall (Villefranche, France). Plasmids were amplified and linearized and mRNA was made using Ambion mMessage mMachine T3 or T7 according to the manufacturer's instructions. Polyadenylated RNA was delivered using a microinjection apparatus consisting of Narishige micromanipulators mounted on a Leica DMI4000 inverted microscope. A microinjection pipette was passed into the ooplasm with the aid of a brief pulse of negative capacitance, applied using an intracellular electrometer (World Precision Instruments). A controlled delivery of ~5% oocyte volume was delivered using a picopump.

Imaging and Analysis

Live epifluorescence imaging of spindle dynamics was carried out on a Leica DMI4000 inverted microscope fitted with a charge-coupled device camera controlled using Leica LAS software. Oocytes were exposed to 5 μg/ml Hoechst for 5 s prior to imaging to label DNA. For immunofluorescence, oocytes were fixed using 4% paraformaldehyde for 30 min, permeabilized in 0.025% Triton-X for 10 min, and blocked in PBS containing 3% BSA for 1 hr at 37°C. Where used, cold shock comprised 10 min exposure to ice-cold medium immediately prior to fixation. Antibodies used were CREST serum (a gift from William Earnshaw, University of Edinburgh) and mouse anti-tubulin (Sigma), with fluorescent secondary antibodies as required (Invitrogen). Confocal imaging of fixed samples was performed on a Zeiss LSM 710 confocal microscope.

PAGFP::tubulin experiments were performed on a Zeiss LSM 510 microscope, as previously described [12]. Photoactivation was performed by brief illumination by a 405 blue diode using the "bleach" function in the LSM software. PAGFP images were acquired using a 520 nm long-pass filter. Alexa 594-tubulin (a gift from Paul Chang, Harvard University) was imaged using a 546 nm laser and a 560 nm long-pass emission filter. Hoechst was excited using a 405 nm blue diode, and emitted light was

(Ci–Ciii) Securin oligonucleotides cause chromosome disjunction and spindle elongation. Eggs were microinjected with control-MO or securin-MO 12–13 hr after hCG administration.

(Ci) Typical example oocytes 24 hr after MO microinjection. Note the scattering of chromosomes and spindle elongation caused by securin-MO. The image to the right shows DNA and kinetochores (CREST) in the same securin-MO-injected oocyte, confirming that securin-MO causes sister chromatid disjunction, as expected.

(Cii) Analysis of spindle lengths. The increase in spindle length caused by securin-MO is highly significant (analysis of variance, $p < 0.01$).

(Ciii) Examples of oocytes cold treated prior to fixation. Note that the MT-staining image brightness has been increased in the securin-MO example to allow visualization of the faint MT structure that persists after cold treatment.

Scale bars represent 10 μm, except inset scale bar in (A), which represents 5 μm. Error bars indicate SEM.

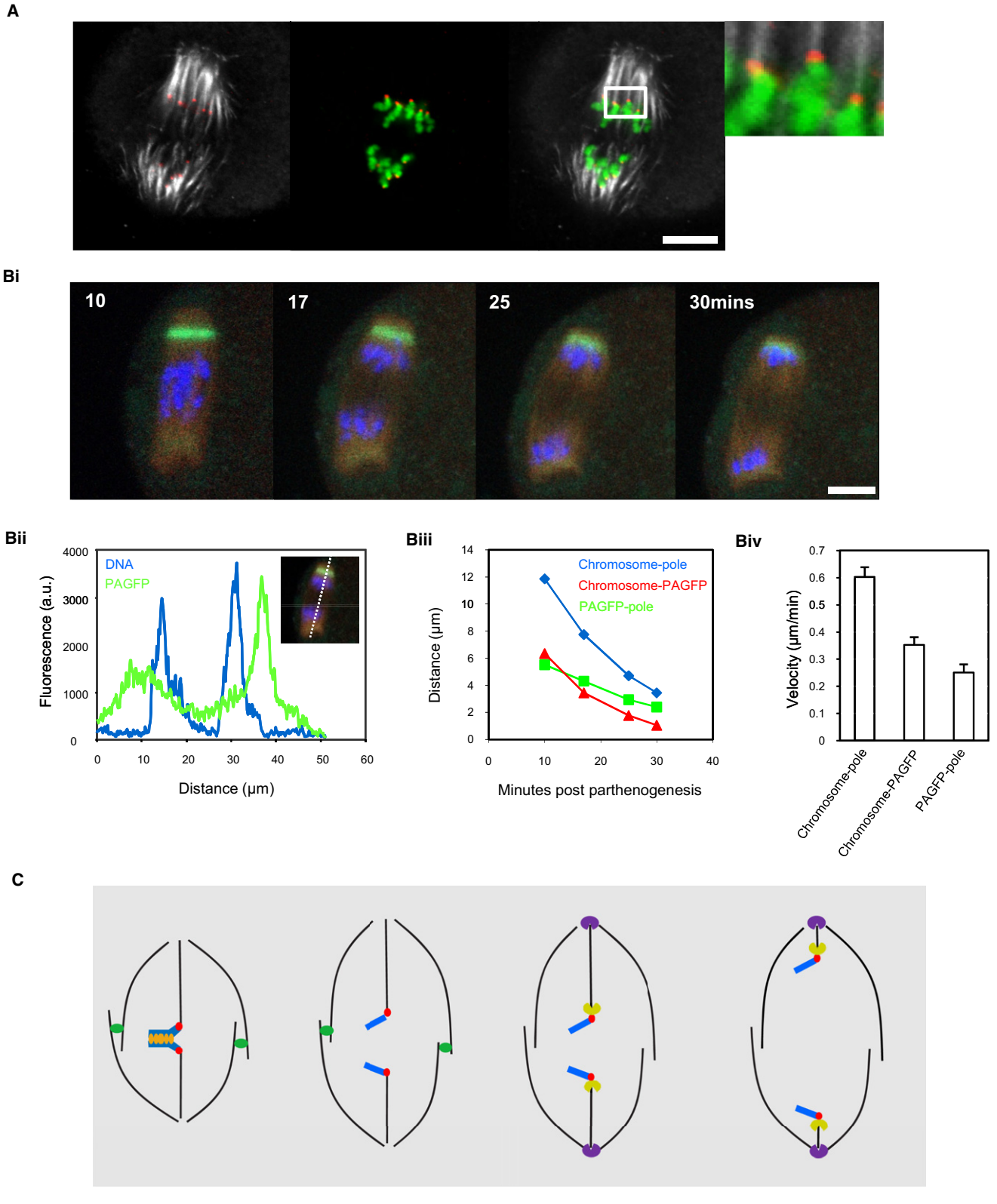

Figure 4. Mechanism of Anaphase A in Mouse Eggs

(A) A spindle in an egg fixed and immunolabeled after cold-shock treatment in anaphase. Note that CREST-labeled kinetochores (red) are at the leading edge of the chromosome (green), at the interface between the chromosome and cold-stable MT fibers (gray) emanating from the spindle pole. Inset shows zoomed overlay of the area indicated by the box.

(Bi) Analysis of anaphase spindle MT dynamics using PAGFP::tubulin (green) and Alexa 594-labeled tubulin (red). A line of PAGFP::tubulin was photoactivated between the spindle pole and anaphase chromosomes (blue), and images were acquired thereafter. Note that as the chromosomes move toward the spindle pole, the distance between the PAGFP line and the pole shortens, as does the distance between the PAGFP line and the chromosomes.

collected with a 420–480 nm band-pass filter. The first image was acquired ~1 min after photoactivation.

Supplemental Information

Supplemental Information includes two figures and can be found with this article online at doi:10.1016/j.cub.2012.01.041.

Acknowledgments

This work was funded by a New Investigator Grant from the Medical Research Council (UK). G.F. thanks John Carroll, Helder Maiato, and Hayden Homer for comments on the manuscript.

Received: December 1, 2011
Revised: January 14, 2012
Accepted: January 20, 2012
Published online: February 16, 2012

References

1. Inoué, S., and Ritter, H., Jr. (1975). Dynamics of mitotic spindle organization and function. Soc. Gen. Physiol. Ser. *30*, 3–30.
2. Maiato, H., and Lince-Faria, M. (2010). The perpetual movements of anaphase. Cell. Mol. Life Sci. *67*, 2251–2269.
3. Ris, H. (1949). The anaphase movement of chromosomes in the spermatocytes of the grasshopper. Biol. Bull. *96*, 90–106.
4. Brust-Mascher, I., and Scholey, J.M. (2002). Microtubule flux and sliding in mitotic spindles of Drosophila embryos. Mol. Biol. Cell *13*, 3967–3975.
5. Brust-Mascher, I., Civelekoglu-Scholey, G., Kwon, M., Mogilner, A., and Scholey, J.M. (2004). Model for anaphase B: role of three mitotic motors in a switch from poleward flux to spindle elongation. Proc. Natl. Acad. Sci. USA *101*, 15938–15943.
6. Azoury, J., Lee, K.W., Georget, V., Rassinier, P., Leader, B., and Verlhac, M.H. (2008). Spindle positioning in mouse oocytes relies on a dynamic meshwork of actin filaments. Curr. Biol. *18*, 1514–1519.
7. Schuh, M., and Ellenberg, J. (2008). A new model for asymmetric spindle positioning in mouse oocytes. Curr. Biol. *18*, 1986–1992.
8. Li, H., Guo, F., Rubinstein, B., and Li, R. (2008). Actin-driven chromosomal motility leads to symmetry breaking in mammalian meiotic oocytes. Nat. Cell Biol. *10*, 1301–1308.
9. Woolner, S., O'Brien, L.L., Wiese, C., and Bement, W.M. (2008). Myosin-10 and actin filaments are essential for mitotic spindle function. J. Cell Biol. *182*, 77–88.
10. Kapoor, T.M., Mayer, T.U., Coughlin, M.L., and Mitchison, T.J. (2000). Probing spindle assembly mechanisms with monastrol, a small molecule inhibitor of the mitotic kinesin, Eg5. J. Cell Biol. *150*, 975–988.
11. Miyamoto, D.T., Perlman, Z.E., Burbank, K.S., Groen, A.C., and Mitchison, T.J. (2004). The kinesin Eg5 drives poleward microtubule flux in Xenopus laevis egg extract spindles. J. Cell Biol. *167*, 813–818.
12. Fitzharris, G. (2009). A shift from kinesin 5-dependent metaphase spindle function during preimplantation development in mouse. Development *136*, 2111–2119.
13. Blangy, A., Lane, H.A., d'Hérin, P., Harper, M., Kress, M., and Nigg, E.A. (1995). Phosphorylation by p34cdc2 regulates spindle association of human Eg5, a kinesin-related motor essential for bipolar spindle formation in vivo. Cell *83*, 1159–1169.
14. Cameron, L.A., Yang, G., Cimini, D., Canman, J.C., Kisurina-Evgenieva, O., Khodjakov, A., Danuser, G., and Salmon, E.D. (2006). Kinesin 5-independent poleward flux of kinetochore microtubules in PtK1 cells. J. Cell Biol. *173*, 173–179.
15. Kollu, S., Bakhoum, S.F., and Compton, D.A. (2009). Interplay of microtubule dynamics and sliding during bipolar spindle formation in mammalian cells. Curr. Biol. *19*, 2108–2113.
16. Schuh, M., and Ellenberg, J. (2007). Self-organization of MTOCs replaces centrosome function during acentrosomal spindle assembly in live mouse oocytes. Cell *130*, 484–498.
17. Mayer, T.U., Kapoor, T.M., Haggarty, S.J., King, R.W., Schreiber, S.L., and Mitchison, T.J. (1999). Small molecule inhibitor of mitotic spindle bipolarity identified in a phenotype-based screen. Science *286*, 971–974.
18. Goshima, G., Saitoh, S., and Yanagida, M. (1999). Proper metaphase spindle length is determined by centromere proteins Mis12 and Mis6 required for faithful chromosome segregation. Genes Dev. *13*, 1664–1677.
19. Bouck, D.C., and Bloom, K. (2007). Pericentric chromatin is an elastic component of the mitotic spindle. Curr. Biol. *17*, 741–748.
20. Goshima, G., Wollman, R., Stuurman, N., Scholey, J.M., and Vale, R.D. (2005). Length control of the metaphase spindle. Curr. Biol. *15*, 1979–1988.
21. Oegema, K., Desai, A., Rybina, S., Kirkham, M., and Hyman, A.A. (2001). Functional analysis of kinetochore assembly in Caenorhabditis elegans. J. Cell Biol. *153*, 1209–1226.
22. Goshima, G., and Scholey, J.M. (2010). Control of mitotic spindle length. Annu. Rev. Cell Dev. Biol. *26*, 21–57.
23. Dumont, S., and Mitchison, T.J. (2009). Force and length in the mitotic spindle. Curr. Biol. *19*, R749–R761.
24. Mitchison, T.J., Maddox, P., Gaetz, J., Groen, A., Shirasu, M., Desai, A., Salmon, E.D., and Kapoor, T.M. (2005). Roles of polymerization dynamics, opposed motors, and a tensile element in governing the length of Xenopus extract meiotic spindles. Mol. Biol. Cell *16*, 3064–3076.
25. Waters, J.C., Skibbens, R.V., and Salmon, E.D. (1996). Oscillating mitotic newt lung cell kinetochores are, on average, under tension and rarely push. J. Cell Sci. *109*, 2823–2831.
26. Maddox, P., Straight, A., Coughlin, P., Mitchison, T.J., and Salmon, E.D. (2003). Direct observation of microtubule dynamics at kinetochores in Xenopus extract spindles: implications for spindle mechanics. J. Cell Biol. *162*, 377–382.
27. Nasmyth, K., and Haering, C.H. (2009). Cohesin: its roles and mechanisms. Annu. Rev. Genet. *43*, 525–558.
28. Hagting, A., Den Elzen, N., Vodermaier, H.C., Waizenegger, I.C., Peters, J.M., and Pines, J. (2002). Human securin proteolysis is controlled by the spindle checkpoint and reveals when the APC/C switches from activation by Cdc20 to Cdh1. J. Cell Biol. *157*, 1125–1137.
29. Nabti, I., Reis, A., Levasseur, M., Stemmann, O., and Jones, K.T. (2008). Securin and not CDK1/cyclin B1 regulates sister chromatid disjunction during meiosis II in mouse eggs. Dev. Biol. *321*, 379–386.
30. Marangos, P., and Carroll, J. (2008). Securin regulates entry into M-phase by modulating the stability of cyclin B. Nat. Cell Biol. *10*, 445–451.
31. Wheatley, S.P., Hinchcliffe, E.H., Glotzer, M., Hyman, A.A., Sluder, G., and Wang, Y. (1997). CDK1 inactivation regulates anaphase spindle dynamics and cytokinesis in vivo. J. Cell Biol. *138*, 385–393.
32. Zhai, Y., Kronebusch, P.J., and Borisy, G.G. (1995). Kinetochore microtubule dynamics and the metaphase-anaphase transition. J. Cell Biol. *131*, 721–734.

(Bii) The locations of peak fluorescence on intensity line scans were used to analyze the relative locations of the PAGFP bar and chromosomes during anaphase.
(Biii) Analyses of the example in (Bi). A shortening of the PAGFP bar-to-pole distance (indicative of disassembly at the pole) and of the chromosome-to-PAGFP bar distance (indicative of pacman) was evident in all experimental replicates (n = 10).
(Biv) Comparison of the velocity of chromosome-pole motion, chromosome-PAGFP motion, and PAGFP-pole movement across all ten experimental replicates. Note that the velocity of chromosome-PAGFP movement is greater than PAGFP-pole movement, suggesting a substantial contribution for MT disassembly at kinetochores.
(C) Cartoon model of the major events of chromosome segregation in the mouse egg. Note that the first phase of chromosome segregation is triggered by loss of cohesin (orange), which triggers a spindle elongation dependent upon kinesin-5 (green), which in turn separates sister chromatids (blue). k-fiber shortening predominantly occurs subsequent to spindle elongation and is the result of MT disassembly both at the kinetochore end (yellow) of the k-fiber and at the pole (purple).
Scale bars represent 10 μm. Error bars indicate SEM.

33. Mitchison, T.J., and Salmon, E.D. (1992). Poleward kinetochore fiber movement occurs during both metaphase and anaphase-A in newt lung cell mitosis. J. Cell Biol. *119*, 569–582.
34. Rogers, G.C., Rogers, S.L., Schwimmer, T.A., Ems-McClung, S.C., Walczak, C.E., Vale, R.D., Scholey, J.M., and Sharp, D.J. (2004). Two mitotic kinesins cooperate to drive sister chromatid separation during anaphase. Nature *427*, 364–370.
35. Rogers, G.C., Rogers, S.L., and Sharp, D.J. (2005). Spindle microtubules in flux. J. Cell Sci. *118*, 1105–1116.
36. Chen, W., and Zhang, D. (2004). Kinetochore fibre dynamics outside the context of the spindle during anaphase. Nat. Cell Biol. *6*, 227–231.
37. Desai, A., Maddox, P.S., Mitchison, T.J., and Salmon, E.D. (1998). Anaphase A chromosome movement and poleward spindle microtubule flux occur At similar rates in Xenopus extract spindles. J. Cell Biol. *141*, 703–713.
38. LaFountain, J.R., Jr., Cohan, C.S., Siegel, A.J., and LaFountain, D.J. (2004). Direct visualization of microtubule flux during metaphase and anaphase in crane-fly spermatocytes. Mol. Biol. Cell *15*, 5724–5732.
39. Tulu, U.S., Rusan, N.M., and Wadsworth, P. (2003). Peripheral, non-centrosome-associated microtubules contribute to spindle formation in centrosome-containing cells. Curr. Biol. *13*, 1894–1899.
40. Hassold, T., and Hunt, P. (2001). To err (meiotically) is human: the genesis of human aneuploidy. Nat. Rev. Genet. *2*, 280–291.
41. Chiang, T., Schultz, R.M., and Lampson, M.A. (2012). Meiotic origins of maternal age-related aneuploidy. Biol. Reprod. *86*, 1–7.
42. Dumont, J., Oegema, K., and Desai, A. (2010). A kinetochore-independent mechanism drives anaphase chromosome separation during acentrosomal meiosis. Nat. Cell Biol. *12*, 894–901.